Particuology 20 (2015) 24–31

Contents lists available at ScienceDirect

Particuology

journal homepage: www.elsevier.com/locate/partic

# Mass and isotopic concentrations of water-insoluble refractory carbon in total suspended particulates at Mt. Waliguan Observatory (China)

Xiangdong Zheng[a,*], Chengde Shen[b], Guojiang Wan[c], Jie Tang[d], Kexin Liu[e]

[a] Key Laboratory of Atmospheric Chemistry, Chinese Academy of Meteorological Sciences, Beijing 100081, China
[b] State Key Laboratory of Isotope Geochronology and Geochemistry, Guangzhou Institute of Geochemistry, Chinese Academy of Sciences, Guangzhou 510640, China
[c] State Key Laboratory of Environment Geochemistry, Institute of Geochemistry, Chinese Academy of Sciences, Guiyang 550002, China
[d] Center of Meteorological Sounding, Chinese Meteorological Administration, Beijing 100081, China
[e] State Key Laboratory of Nuclear Physics and Technology and Institute of Heavy Ion Physics, Peking University, Beijing 100871, China

ARTICLE INFO

*Article history:*
Received 25 May 2014
Received in revised form 31 October 2014
Accepted 4 November 2014

*Keywords:*
Water-insoluble refractory carbon (WIRC)
Mass concentration
$\delta^{13}C$
$^{14}C$
Mt. Waliguan (WLG)

ABSTRACT

Mass concentration and isotopic values $\delta^{13}C$ and $^{14}C$ are presented for the water-insoluble refractory carbon (WIRC) component of total suspended particulates (TSP), collected weekly during 2003, as well as from October 2005 to May 2006 at the WMO-GAW Mt. Waliguan (WLG) site. The overall average WIRC mass concentration was $(1183 \pm 120)$ ng/m$^3$ ($n = 79$), while seasonal averages were $2081 \pm 1707$ (spring), $454 \pm 205$ (summer), $650 \pm 411$ (autumn), and $1019 \pm 703$ (winter) ng/m$^3$. Seasonal variations in WIRC mass concentrations were consistent with black carbon measurements from an aethalometer, although WIRC concentrations were typically higher, especially in winter and spring. The $\delta^{13}C$ PDB value ($-25.3 \pm 0.8$)‰ determined for WIRC suggests that its sources are $C_3$ biomass or fossil fuel combustion. No seasonal change in $\delta^{13}C$ PDB was evident. The average percent Modern Carbon (pMC) for $^{14}C$ in WIRC for winter and spring was $(67.2 \pm 7.7)$% ($n = 29$). Lower pMC values were associated with air masses transported from the area east of WLG, while higher pMC values were associated with air masses from the Tibetan Plateau, southwest of WLG. Elevated pMC values with abnormally high mass concentrations of TSP and WIRC were measured during a dust storm event.



## Introduction

Carbonaceous aerosols are usually separated into organic carbon (OC) and elemental carbon (EC) fractions using thermal oxidation techniques. OC, oxidized at temperatures lower than 400 °C, is directly emitted from its primary source, or composed of secondary organic aerosols (SOA) formed through condensation and particulate conversion of hydrocarbon gas phase oxidation products. OC is also one of the main components of fine particulate matter, with an aerodynamic radius less than 2.5 μm ($PM_{2.5}$). In contrast, EC is emitted during oxygen-deficient combustion of biomass or fossil fuels, and covers a continuum from charcoal (or char) to soot particles (Hedges et al., 2000). Its chemical and physical properties are relatively inert. Black carbon (BC) measured by optical instruments, such as an aethalometer, is comparable with EC in its thermal, optical, and chemical behavior.

Carbonaceous aerosols may also be differentiated into water soluble and insoluble types based on their water-solubilities at a given temperature and pressure. Water-soluble organic carbon (WSOC) constitutes a significant fraction of fine carbonaceous particulate matter, having complicated molecular compositions of oxidized and hygroscopic materials (Novakov & Penner, 1993). In contrast, water-insoluble carbon in aerosol particles is refractory, incorporating oxidized and hydrophobic materials like EC and water-insoluble organic carbon (WIOC). Large aromatics ($\geq C_9$), lignin, and cellulose are the main compounds of WIOC (Saxena & Hildemann, 1996).

Carbon isotope technology provides a simple but effective method for EC and OC source apportionment. Stable $^{13}C$ isotope ratios are characteristic of different aerosol sources, while radioactive $^{14}C$ concentrations can differentiate modern biogenic-derived versus fossil fuel-derived carbonaceous matters because

* Corresponding author. Tel.: +86 1058995272; fax: +86 10 62186414.
*E-mail address:* zhengxd@cams.cma.gov.cn (X. Zheng).

http://dx.doi.org/10.1016/j.partic.2014.11.003
1674-2001/

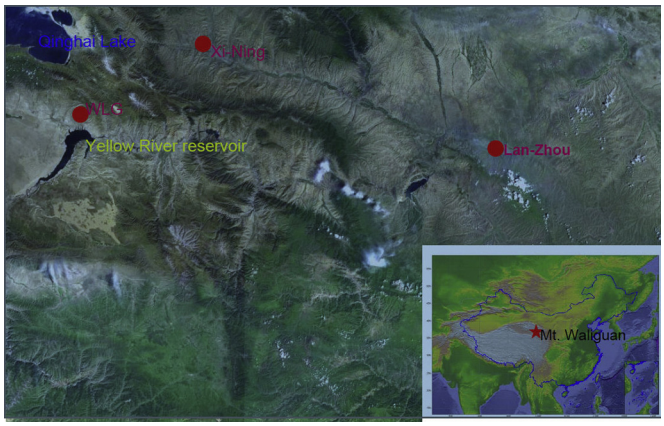


**Fig. 1.** Topographical map of Mt. Waliguan (WLG) showing the study site and surrounding regions.

$^{14}C$ only exists in the contemporary biogenic-derived material (Currie, Klouda, & Cooper, 1980). Thus, $^{14}C$ measurements have vastly improved our understanding of $PM_{2.5}$ sources (e.g. Bench, Fallon, Schichtel, Malm, & McDade, 2007; Gustafsson et al., 2009; Heal et al., 2011; Sun, Hu, Guo, Liu, & Zhou, 2012; Szidat et al., 2004, 2006). In this study, we express $^{14}C$ in percent Modern Carbon (pMC).

Mt. Waliguan (36.287° N, 100.898° E; 3810 m AMSL; hereafter WLG) Observatory, one of 22 World Meteorological Organization-Global Atmosphere Watch (WMO-GAW) sites, is located on a remote mountaintop in the northeast region of the Tibetan Plateau. Fig. 1 shows the geographical and topographical context of WLG. The provincial capital cities, Lanzhou and Xining, are respectively about 270 and 90 km from WLG. It is important to explore sources of aerosol particles at this WMO-GAW site, since it is less influenced by anthropogenic pollution compared with most Asian sites. It has been demonstrated that aerosol particles at WLG mainly consist of WSOC, carbonate ($CaCO_3$), and $NH_4SO_4$ (Li, Tang, Xue, & Toom-Sauntry, 2000). Regional transport of air pollution from Lanzhou and Xining, as well as from east China contribute to BC levels at WLG, as reported by Tang et al. (1999). In addition, soil, crustal material, emissions from coal burning, vehicles, and industry are identified as primary sources of aerosols at WLG (Wen, Xu, Tang, Zhang, & Zhao, 2001). Biomass burning also is a significant primary source, as suggested by a correlation between BC with $NO_3^-$, $K^+$, $NH_4^+$, $Ca^{2+}$, and $Mg^{2+}$ ions (Ma, Tang, Li, & Jacobson, 2003). Although particle size distributions suggest that air masses from west of WLG are dominant at this site, regional-scale transport from the northeast, including emissions from Xining and Lanzhou, frequently brings major anthropogenic pollutants with particle sizes in the Aitken mode (21 nm < $d_p$ < 95 nm) and accumulation mode (95 nm < $d_p$ <570 nm) during summer (Kivekäs et al., 2009).

In this study, characteristics of carbon materials extracted from total suspended particulates (TSP) collected weekly at WLG are determined. TSP samples were collected over two periods: from December 25, 2002 to January 21, 2004; and from October 16, 2005 to May 17, 2006. Samples were measured for $^{10}Be$ and carbon isotopes, after $^{7}Be$ and $^{210}Pb$ were determined without damage to the original samples. Since samples were originally collected for $^{7}Be$ and $^{210}Pb$ analysis, a special procedure (see "Experimental" section), somewhat different from chemical-thermal oxidation techniques applied to aerosol particles collected on quartz filters, was used for extracting carbon in this study.

## Experimental

### *Sample collection*

TSP were collected using a high volume air sampler driven by Fuji-Electric Co (Japan) pumper (Model:VFC404p-5T), with a rectangular filter composed of three layers of 100% polypropylene web (Dynaweb DW7301L, 25.4 cm × 20.3 cm) (Lee et al., 2004). A flow rate of ca. 1.2 $m^3$/min was used. The sampling period was set to one week (168 h). Although the optimal size of particles is larger than 0.4 μm, our high volume sampling system collected TSP composed of differently sized particles, including pollen grains with sizes between 2.5 and 10.0 μm (Pavuluri, Kawamura, Uchida, Kondo, & Fu, 2013). For the first sample period, only three eighths of each filter was available for carbon extraction.

### *Sample pretreatments*

A modified 3A (acid–alkali–acid) treatment was used to extract carbon, similar to the procedures used to extract BC from soil or marine sediments (e.g., Han et al., 2007; Khan et al., 2009) or from archived aerosol filter samples (Husain et al., 2008). The first acid treatment separates particles attached to the polypropylene fibers. This procedure involves soaking the filter in 6 M HCl solution at room temperature for 24 h, and then the extracted insoluble TSP materials are precipitated or floated, which are collected and washed to pH = 7.0 with deionized water before being dried. During the alkali treatment, these insoluble particles are soaked in 1 M NaOH solution at room temperature for 24 h. This removes humic-like substances from solids. The residues are collected by filtration, and washed to pH = 7.0 with deionized water prior to being dried for the last acid treatment. The final treatment eliminates any possible secondary carbonate produced in the first two treatments.

After these treatments, the dried residue is placed in a Vycors® combustion tube packed with pre-heated CuO and silver wire. The combustion tube is held under vacuum conditions with pressure around $1 \times 10^{-3}$ hPa for 3 h, before being sealed by liquefied gas-oxygen flame welding. Thus, all volatile and semi-volatile organic substances are removed, leaving only stable recalcitrant carbonaceous matter. Although the attributes of this carbonaceous material are similar to BC chemically extracted from soil or marine sediments (e.g. Khan et al., 2009), we prefer to use the term water-insoluble refractory carbon (WIRC) because of the differences in its extraction method compared with traditional methods used for quartz or Teflon-filters.

### *Conversion to $CO_2$ and graphite target synthesis*

The sealed tube of WIRC is combusted at 860 °C for 2 h in a muffle oven, and the carbon-containing gases evolving from the residue are converted to $CO_2$. The $CO_2$ is released into a cracker tube under vacuum conditions to determine the mass concentration of WIRC using $CO_2$ partial pressure measurements. The $CO_2$ is introduced to a dry ice ethanol-trap to eliminate water vapor, before it is cryogenically trapped using a liquid $N_2$ trap. The trapped $CO_2$ is divided into two parts: one is sealed in a tube for $^{13}C$ measurement, and the other is reintroduced into the dry ice ethanoland liquid $N_2$ traps 2–3 times to obtain more purified $CO_2$. This purified $CO_2$ is converted to graphite at 600 °C using zinc with iron, and a $TiH_2$ catalyst in excess hydrogen. This produces targets for $^{14}C$ analysis. Procedures for carbon separation, purification, and target synthesis are described in the literature (Ding et al., 2010; Shen et al., 1999).

**Table 1**
Uncertainty investigations of WIRC mass concentration, $\delta^{13}C$ PDB, and $^{14}C$ pMC.

| | Known | Estimated | Unknown |
|---|---|---|---|
| Mass conc. | ~±5% | Volume calculation ~±5%, or >±5% in the summer–autumn 2003; ~20% WIRC loss during the chemical extraction procedures | Kerogen contribution; cutting of filter |
| $\delta^{13}C$ PDB | ~±0.2‰ | | Kerogen contribution |
| $^{14}C$ pMC | ~±1% | Correction factor ~3 ± 6% | As for $\delta^{13}C$ PDB |

*$^{13}C$ and $^{14}C$ measurements*

$^{13}C$ is expressed as value of $\delta^{13}C$, i.e., the ratio $^{13}C/^{12}C$ in the sample compared with that in the international standard Pee Dee Belemnite (PDB), as given by:

$$\delta^{13}C = \left[\frac{^{13}C/^{12}C_{sample}}{^{13}C/^{12}C_{standard}} - 1\right] \times 1000\ ‰\ . \quad (1)$$

In this study, $\delta^{13}C$ was determined by a Finnigan Model-251 mass spectrometer (Thermo Electron Corporation, USA). For each sample, duplicate analyses were performed. A $\delta^{13}C$ value was only accepted, when its difference from its replicate was less than 0.1‰. Analysis of blank filters provided a filter blank correction in terms of absolute values, which amounted to ±0.2‰ on average.

$^{14}C$ is expressed as the fraction of modern carbon (pMC), which is determined by comparing the observed $^{14}C$ content in the sample with that in a standard, as defined below:

$$pMC = \frac{(^{14}C/^{12}C)_{sample}}{0.95(^{14}C/^{12}C)_{OXI}} \times 100\%, \quad (2)$$

where $(^{14}C/^{12}C)_{OXI}$ is the ratio for the US-NIST oxalic acid standard I (NBS OxI). The ratios of $^{14}C/^{12}C$ in our graphite targets were measured by an updated NEC Compact Accelerator Mass Spectrometry (AMS; National Electrostatics Corporation, WI, USA), with sensitivity less than $6 \times 10^{-15}$ and accuracy better than 1.0% at the Peking University (Liu et al., 2007). The AMS calibration suggests that the value for a blank is 0.4–0.5% (Sun et al., 2012).

Because of above-ground nuclear testing before the 1960s, excessive ambient $^{14}C$ from bomb tests must be corrected. For biogenic emissions, a value of 1.04 was used by Levin, Hammer, Kromer, and Meinhardt (2008). Szidat et al. (2009) recommended a ratio of 1.16 for 30–50-year old trees. A factor of 1.08 was proposed by Bench et al. (2007), and also was adopted for $PM_{2.5}$ samples collected at a rural site in Beijing (Sun et al., 2012). In this study, we use a factor of 1.1, which was the pMC value for TSP collected at Lhasa (Huang et al., 2010). This allows pMC values to be easily compared between WLG and Lhasa, since they were determined by similar methods, except that quartz and Teflon filters were used in Lhasa (Huang et al., 2010).

*Uncertainty of the data*

Table 1 presents a summary of measurement uncertainty in our study. Known uncertainty caused by instrument precision was estimated from public references, that is, uncertainties for mass concentration, $\delta^{13}C$ PDB, and $^{14}C$ pMC were ±5% (Shen et al., 1999), ±0.2‰ (Ding et al., 2010), and ±1% (Liu et al., 2007), respectively.

Highest uncertainty was for mass concentration. There were at least three sources of uncertainty for WIRC mass concentration: (i) sample volume estimation; (ii) loss of TSP in pretreatment procedures; and (iii) the influence of kerogen on the insoluble organic material fraction. During a 7-day sampling period, the record of flow-rate was too sparse to evaluate accurate sample volumes. This contributes to an uncertainty of about ±5%. This uncertainty was greater when volumes were low from summer to autumn of 2003 (Table 2). Another issue with volume estimation is that the sample filter was cut, and only 3/8 of a sample was used for carbonaceous extraction for the first 56 samples. Large volume differences occurred between the first 56 and the later 29 samples (Tables 2 and 3). Contributions to uncertainty also were related to pretreatment practices. After the first acid treatment, the surface of the discarded polypropylene filter was still stained, indicating that some fine carbonaceous particles embedded in the filter were unrecoverable. The total recovery efficiency is roughly estimated to be 80%, much lower than for $ZnCl_2$-dissolution methods for Whatman 41 filters ((93 ± 4)%) described by Li, Khan, and Husain (2002). Fortunately, carbon isotope analyses are not overly influenced by small losses of WIRC (e.g., Bench et al., 2007). Kerogen in the aerosol samples can be removed using $K_2Cr_2O_7 + H_2SO_4$ during the pretreatment (e.g., Husain et al., 2008; Khan et al., 2009). This separation procedure was not carried out in this study, since we envisaged that it would be a positive input for WIRC mass concentration and a negative one for pMC values.

The correction factor applied in Eq. (2) introduces additional uncertainty for pMC values. The factor of 1.1 used in this study introduces at least (3 ± 6)% uncertainty, if the recommended factor of 1.08 ± 0.06 is used as a baseline (Bench et al., 2007; Heal et al., 2011; Sun et al., 2012).

## Results and discussion

*Mass concentration*

Highest TSP mass concentrations, with more than 50 μg/m$^3$, occurred in winter and spring samples (Tables 2 and 3). In the moist summer to autumn period, TSP concentration also was typically higher than 5 μg/m$^3$. These values are much higher than background TSP levels at other GAW sites, such as Jungfraujoch in the Swiss Alps (Collaud Coen et al., 2004) or Alert in the Arctic (Kuhn, Damoah, Bacak, & Sloan, 2010), where TSP concentrations are around 0.8 μg/m$^3$ and 0.05–3 μg/m$^3$, respectively. These comparisons suggest a highly TSP-laden background signal exists at WLG.

Mass concentrations of WIRC were also high at WLG. The overall mean mass concentration was (1183 ± 120) ng/m$^3$ ($n$ = 79). While seasonal mean concentrations were 2081 ± 1707 ($n$ = 24, spring), 454 ± 205 ($n$ = 11, summer), 650 ± 411 ($n$ = 17, autumn), and 1019 ± 703 ng/m$^3$ ($n$ = 27, winter). The relatively low WIRC concentrations in summer to autumn are related to frequent occurrences of cloud or fog that permits aged aerosol particles to be wet and scavenged (rained out) on the mountaintop. In addition, abundant precipitation directly washes out aerosol particles in WLG and its surrounding regions. These removal processes create a shorter residence time for near surface aerosol particles at this site. In the contrast, low amounts of precipitation during the dry winter to spring period results in buildup of higher mass concentrations of TSP, as well as WIRC.

The overall mean WIRC/TSP ratio was (2.25 ± 1.3)%, while seasonal averages were (1.9 ± 0.7)% (spring), (2.86 ± 1.3)% (summer), (2.96 ± 1.5)% (autumn), and (2.25 ± 1.1)% (winter). Higher WIRC mass ratios in summer and autumn suggest a reduced dust-soil fraction in the TSP. This reflects seasonal precipitation that depresses continental emissions of aerosol particles, as well as air parcels transported from the more urbanized areas, east of WLG.

**Table 2**
Sampling records, mass concentrations of TSP and WIRC, and $\delta^{13}C$ PDB values at WLG from December 2002 until January 2004.

| Sample No. | Sampling date | | Volume ($m^3$) | TSP conc. ($\mu g/m^3$) | WIRC conc. ($ng/m^3$) | $\delta^{13}C$ PDB (‰) |
|---|---|---|---|---|---|---|
| | Start YY-MM-DD | End YY-MM-DD | | | | |
| WLG-1 | 02-12-25 | 03-01-01 | 2445 | 20.65 | 526.4 | −25.08 |
| WLG-2 | 03-01-01 | 03-01-08 | 2547 | 31.02 | 331.7 | −25.30 |
| WLG-3 | 03-01-08 | 03-01-15 | 2402 | 24.31 | 69.3 | −25.41 |
| WLG-4 | 03-01-15 | 03-01-22 | 2439 | 19.72 | 341.4 | −25.13 |
| WLG-5 | 03-01-22 | 03-01-29 | 2415 | 50.68 | 248.7 | −25.77 |
| WLG-7 | 03-02-05 | 03-02-12 | 2431 | 72.30 | 1381.9 | −24.86 |
| WLG-8 | 03-02-12 | 03-02-19 | 1956 | 77.03 | 1248.5 | −24.85 |
| WLG-11 | 03-03-05 | 03-03-12 | 1970 | 225.40 | 2316.8 | −24.80 |
| WLG-12 | 03-03-12 | 03-03-19 | 2248 | 60.45 | 1024.5 | −24.67 |
| WLG-13 | 03-03-19 | 03-03-26 | 2244 | 76.25 | 1297.0 | −25.02 |
| WLG-14 | 03-03-26 | 03-04-02 | 2083 | 113.12 | 1647.6 | −24.97 |
| WLG-15 | 03-04-02 | 03-04-09 | 2235 | 81.89 | 1138.7 | −24.64 |
| WLG-16 | 03-04-09 | 03-04-16 | 1236 | 485.42 | 3708.2 | −24.73 |
| WLG-17 | 03-04-16 | 03-04-23 | 1433 | 346.16 | 1112.3 | −24.83 |
| WLG-18 | 03-04-23 | 03-04-30 | 2121 | 97.53 | 1139.3 | −25.05 |
| WLG-19 | 03-04-30 | 03-05-07 | 2251 | 48.02 | 377.6 | −25.59 |
| WLG-20 | 03-05-07 | 03-05-14 | 2330 | 72.18 | 708.9 | −23.40 |
| WLG-21 | 03-05-14 | 03-05-21 | 2314 | 30.89 | 549.5 | −24.90 |
| WLG-22 | 03-05-21 | 03-05-25 | 1422 | 14.91 | 106.5 | −28.00 |
| WLG-23 | 03-05-28 | 03-06-04 | 2352 | 36.70 | 798.4 | −25.07 |
| WLG-24 | 03-06-04 | 03-06-10 | 2012 | 7.80 | 254.9 | −25.22 |
| WLG-26 | 03-06-18 | 03-06-25 | 2283 | 20.14 | 717.8 | −25.53 |
| WLG-27 | 03-06-25 | 03-07-28 | 943 | 30.33 | 511.0 | −25.13 |
| WLG-28 | 03-07-02 | 03-07-09 | 2283 | 17.66 | 291.5 | −25.33 |
| WLG-29 | 03-07-09 | 03-07-12 | 948 | 5.80 | 124.1 | −25.44 |
| WLG-30 | 03-07-16 | 03-07-23 | 2289 | 16.60 | 266.5 | −25.13 |
| WLG-31 | 03-07-23 | 03-07-29 | 2095 | 11.31 | 419.2 | −25.64 |
| WLG-32 | 03-07-30 | 03-08-06 | 2043 | 12.38 | 326.2 | −25.18 |
| WLG-33 | 03-08-06 | 03-08-09 | 1168 | 5.57 | 261.5 | −25.47 |
| WLG-34 | 03-08-13 | 03-08-20 | 2182 | 42.26 | 769.1 | −25.68 |
| WLG-35 | 03-08-20 | 03-08-27 | 2101 | 7.00 | 380.7 | −25.79 |
| WLG-37 | 03-09-03 | 03-09-10 | 2305 | 6.99 | 262.7 | −25.41 |
| WLG-38 | 03-09-10 | 03-09-16 | 2174 | 9.94 | 413.8 | −25.82 |
| WLG-40 | 03-09-24 | 03-09-29 | 1544 | 2.91 | 83.8 | −25.66 |
| WLG-41 | 03-10-01 | 03-10-08 | 2248 | 6.45 | 117.7 | −25.16 |
| WLG-42 | 03-10-08 | 03-10-11 | 571 | 10.16 | 475.3 | −25.42 |
| WLG-43 | 03-10-15 | 03-10-22 | 2304 | 34.19 | 833.8 | −25.70 |
| WLG-44 | 03-10-22 | 03-10-29 | 2306 | 20.16 | 657.6 | −25.80 |
| WLG-45 | 03-10-29 | 03-11-05 | 2315 | 10.07 | 219.6 | −25.04 |
| WLG-46 | 03-11-05 | 03-11-12 | 2388 | 54.57 | 585.4 | −25.34 |
| WLG-47 | 03-11-12 | 03-11-19 | 2295 | 27.28 | 124.3 | −24.70 |
| WLG-48 | 03-11-19 | 03-11-26 | 2380 | 40.58 | 542.9 | −25.22 |
| WLG-49 | 03-11-26 | 03-12-03 | 2351 | 109.12 | 615.8 | −25.31 |
| WLG-50 | 03-12-03 | 03-12-10 | 2489 | 26.68 | 188.5 | −25.71 |
| WLG-51 | 03-12-10 | 03-12-17 | 2438 | 38.43 | 404.1 | −25.42 |
| WLG-52 | 03-12-17 | 03-12-24 | 2440 | 46.22 | 536.3 | −25.36 |
| WLG-53 | 03-12-24 | 03-12-31 | 2432 | 37.42 | 862.0 | −25.30 |
| WLG-54 | 03-12-31 | 04-01-07 | 2505 | 32.57 | 587.7 | −25.57 |
| WLG-55 | 04-01-07 | 04-01-14 | 2439 | 30.22 | 567.2 | −25.27 |
| WLG-56 | 04-01-14 | 04-01-21 | 2480 | 35.04 | 624.50 | −24.74 |

These air masses are likely to be well mixed, with a high diversity of chemical components, including anthropogenic emissions. For example, pollutants $O_3$ or $NO_X$ are recorded in these air flows (e.g. Lee et al., 2004; Xue et al., 2011). Scatter plots to compare mass concentrations of WIRC and TSP at WLG are shown in Fig. 2. To obtain equivalent sample numbers, data from summer and autumn were grouped together. The linear least-squared fit and squared correlation coefficients suggest a poorer correlation between WIRC and TSP in summer and autumn than in winter and spring. Thus, the source for WIRC at WLG in the summer–autumn period was less dependent on TSP than in the other seasons.

We compared our WIRC mass concentrations with those from Lhasa (Huang et al., 2010), located on the southern Tibetan Plateau at approximately the same altitude above sea level (29.67° N, 91.13° E; 3650 AMSL). In addition, the laboratory measurement techniques used for WIRC-TSP samples at these two sites were similar, except that at Lhasa, TSP was collected on different filters. Absolute and relative mass concentrations of WIRC at Lhasa were $(13{,}740 \pm 5905)\,ng/m^3$ and $(9.5 \pm 4.1)\%$ (Huang et al., 2010), which are markedly higher than those at WLG, even when data uncertainty (more than ~−30%) is taken into account. This shows that TSP and WIRC loadings at WLG are lower than for the Tibetan region.

### *Comparison with aethalometer BC*

The weekly average mass concentrations of WIRC and BC (aethalometer measurements) at WLG show that their seasonal variations were generally consistent (Fig. 3). BC concentrations were close to those for WIRC from May to December 2003, but WIRC concentrations were higher in the winter–spring period, especially in the 29 most recent samples.

**Table 3**
Sampling records, mass concentrations of TSP and WIRC, and $\delta^{13}C$ PDB, $^{14}C$ pMC values at WLG from October 2005 until May 2006.

| Sample No. | Sampling date | | Volume ($m^3$) | TSP conc. ($\mu g/m^3$) | WIRC conc. ($ng/m^3$) | $\delta^{13}C$ PDB (‰) | $^{14}C$ pMC (%) |
|---|---|---|---|---|---|---|---|
| | Start YY-MM-DD | End YY-MM-DD | | | | | |
| #01 | 05-10-26 | 05-11-02 | 5092 | 28.33 | 1497.3 | −25.59 | 60.57 ± 0.22 |
| #02 | 05-11-02 | 05-11-09 | 5070 | 18.64 | 632.2 | −25.5 | 68.08 ± 0.23 |
| #03 | 05-11-09 | 05-11-16 | 5126 | 29.62 | 1325.6 | −25.45 | 56.71 ± 0.20 |
| #04 | 05-11-16 | 05-11-23 | 5237 | 21.79 | 881.3 | −25.54 | 56.31 ± 0.19 |
| #05 | 05-11-23 | 05-11-30 | 5222 | 11.07 | 508.4 | −25.2 | 66.84 ± 0.22 |
| #06 | 05-11-30 | 05-12-07 | 5015 | 24.53 | 886.9 | −25.06 | 75.58 ± 0.24 |
| #07 | 05-12-07 | 05-12-14 | 5030 | 62.92 | 2052.5 | −24.96 | 57.03 ± 0.20 |
| #08 | 05-12-14 | 05-12-21 | 5262 | 19.38 | 713.5 | −24.66 | 74.88 ± 0.26 |
| #09 | 05-12-21 | 05-12-28 | 5130 | 15.76 | 718.1 | −25.57 | 74.61 ± 0.25 |
| #10 | 05-12-28 | 06-01-04 | 4863 | 106.03 | 2471.9 | −25.3 | 73.19 ± 0.25 |
| #11 | 06-01-04 | 06-01-11 | 4482 | 111.88 | 2325.3 | −24.88 | 74.3 ± 0.25 |
| #12 | 06-01-11 | 06-11-18 | 4796 | 63.80 | 1849.3 | −25.07 | 66.53 ± 0.23 |
| #13 | 06-01-18 | 06-01-25 | 5111 | 46.39 | 2129.5 | −24.98 | 54.99 ± 0.22 |
| #14 | 06-01-25 | 06-02-01 | 4357 | 72.21 | 1845.0 | −24.84 | 80.79 ± 0.26 |
| #15 | 06-02-01 | 06-02-08 | 4428 | 65.54 | 1592.3 | −24.67 | 71.34 ± 0.24 |
| #16 | 06-02-08 | 06-02-15 | 5150 | 23.32 | 637.8 | −25.17 | 73.57 ± 0.24 |
| #17 | 06-02-15 | 06-02-22 | 5117 | 48.78 | 1327.5 | −24.87 | 67.79 ± 0.23 |
| #18 | 06-02-22 | 06-03-01 | 5179 | 36.73 | 762.6 | −29.66 | 64.13 ± 0.26 |
| #19 | 06-03-01 | 06-03-08 | 4954 | 37.77 | 1009.8 | −25.07 | 63.39 ± 0.26 |
| #20 | 06-03-08 | 06-03-15 | 4739 | 111.96 | 1596.7 | −24.55 | 67.4 ± 0.23 |
| #21 | 06-03-15 | 06-03-22 | 3839 | 204.95 | 3435.2 | −24.83 | 60.54 ± 0.23 |
| #22 | 06-03-22 | 06-03-29 | 4604 | 86.94 | 2042.8 | −25.03 | 57.53 ± 0.22 |
| #23 | 06-03-29 | 06-04-05 | 4286 | 100.99 | 1929.6 | −24.85 | 67.31 ± 0.25 |
| #24 | 06-04-05 | 06-04-12 | 4508 | 233.48 | 4036.3 | −24.24 | 79.76 ± 0.28 |
| #25 | 06-04-12 | 06-04-19 | 3845 | 170.77 | 1875.1 | −24.83 | 63.1 ± 0.23 |
| #26 | 06-04-19 | 06-04-26 | 4322 | 83.24 | 1572.3 | −24.9 | 61.81 ± 0.21 |
| #27 | 06-04-26 | 06-05-03 | 4715 | 47.47 | 1153.0 | −24.97 | 59.27 ± 0.22 |
| #28 | 06-05-03 | 06-05-10 | 4298 | 62.41 | 636.8 | −24.6 | 63.52 ± 0.21 |
| #29 | 06-05-10 | 06-05-17 | 4832 | 53.14 | 797.6 | −24.87 | 61.24 ± 0.22 |

Scatter plots for WIRC and BC mass concentrations over the two sampling periods are shown in Fig. 4. In the second period for samples without filter cutting, the linear dependence is better than for the first period, when only 3/8 of each filter was used. Obviously, filter cutting and low sample volumes in summer to autumn of 2003 resulted in loss of WIRC mass. However, mass concentrations of WIRC were almost always higher than those for BC. This reflects differences in sampling techniques. The high flow rate (1.2 $m^3$/min) used for TSP sampling in this study collects differently sized carbonaceous particles, with particles up to 10 μm in size (Pavuluri et al., 2013). In contrast, the aethalometer flow rate was only around 8 L/min, and did not collect larger size particles. In winter to spring, higher TSP loadings on the filters resulted in higher mass concentrations of WIRC.

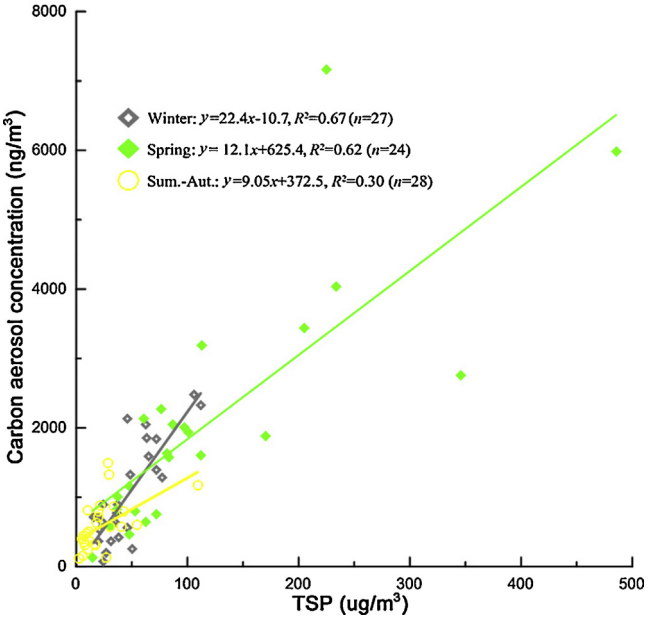


**Fig. 2.** Scatter plot of TSP and WIRC mass concentrations at WLG in winter, spring, and combined summer–autumn data.

### *$\delta^{13}C$ PDB*

The $\delta^{13}C$ values for WIRC at WLG exhibit uniformity (Tables 2 and 3). The mean $\delta^{13}C$ PDB value was (−25.3 ± 0.8)‰ ($n$ = 79), equivalent to $\delta^{13}C$ values for $C_3$ biomass (−24‰ to −34‰) or coal (−22‰ to −28‰) combustion. The mean $\delta^{13}C$ for WLG samples was also close to that measured in Lhasa (−25.8‰) (Huang et al., 2010). Seasonal variation in $\delta^{13}C$ at WLG was not marked. Summer and autumn $\delta^{13}C$ values were close to those measured in silage-fed cattle dung (−25.7 ± 0.4)‰ in tropical India (Pavuluri, Kawamura, Swaminathan, & Tachibana, 2011). Less-depleted $\delta^{13}C$ in spring suggests there was dilution of the heavier isotopic carbon fraction in WIRC.

Notably, there were two cases of extremely low $\delta^{13}C$ values: −28.8‰ was recorded during the interval May 21–25, 2003; while −29.0‰ was recorded during February 22–28, 2006. Such low $\delta^{13}C$ values may reflect particles from a specific WIRC source. In the first instance, a relatively clean air mass was associated with lowest mass concentrations for TSP and WIRC (Table 2) and could be related to enhanced wet scavenging processes during precipitation over the sampling period. In the later instance, the low value was clearly not related to low TSP values or precipitation (Table 3).

We investigated possible source regions for these abnormally low $\delta^{13}C$ values using backward trajectory calculations available online at www.arl.noaa.gov/ready/open/traj.html (Draxler & Rolph, 2003). In the first instance, the air mass transport path was mainly from the east, southeast, and south of WLG, including regions in

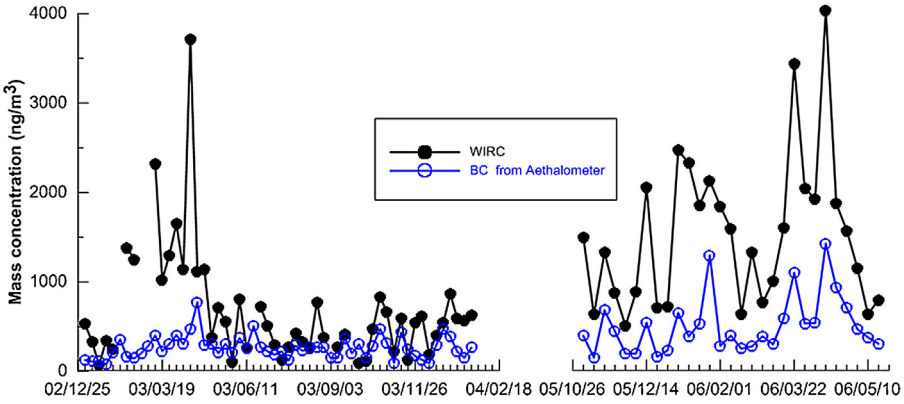


**Fig. 3.** Weekly mass concentrations of WIRC and aethalometer BC at WLG.

Sichuan Province and Chongqin, where oil and gas exploitation occurs. In the later instance, the main air mass transport was from west of WLG, including the Persian Gulf region. These backward trajectories indicate that lowest $\delta^{13}C$ values at WLG were related to regionally transported emissions from the oil and gas industry. The average $\delta^{13}C$ for oil is about −28.0‰, consistent with the low values for our two cases. Our data show that it is difficult to identify source regions for WIRC using only $\delta^{13}C$ data and backward trajectory calculations because one-week continuous TSP samples reflect a variety of aerosol particles that have been mixed along their transport paths, weakening the significance of stable carbon isotopic compositions as tracers for WIRC sources.

### *$^{14}C$ pMC*

The mean value for $^{14}C$ pMC in samples collected from winter 2005 to spring 2006 was (67.2 ± 7.7)% ($n$ = 29). Our $^{14}C$ pMC data are compared with measurements from other sites in China undertaken by the same AMS facility in Table 4. Comparison between WLG and Lhasa values reveals a lower carbon loading related to fossil fuel combustion at WLG. Both Lhasa and WLG show higher contemporary carbon fractions for WIRC than $^{14}C$ pMC in $PM_{2.5}$ from urbanized sites in east China. Lhasa and WLG also had highest $^{14}C$ pMC values in winter (DJF, i.e. December, January, and February).

There are several studies of $^{14}C$ pMC values for $PM_{2.5}$. In the US, pMC values of 50% at urban sites and 70–97% at non-urban sites were reported (Bench et al., 2007; Schichtel et al., 2008). In Europe, data ranged from 57% to 82% for five remote and rural sites (Gelencsér et al., 2007). Clearly, a greater contribution of biogenic carbon to $PM_{2.5}$ was present at all non-urban sites. As a remote GAW site, the WIRC $^{14}C$ pMC value at WLG was even lower than for $PM_{2.5}$ at non-urban sites. Another reason for the low values in our study is that biogenic-derived WSOC were eliminated in the pretreatments. Given its complex composition, WIRC should have the recalcitrant properties of EC or BC. The extraction process for WIRC from the TSP is also similar to that for BC in soil or marine sediments. However, the $^{14}C$ pMC reported here is much higher than for EC in $PM_{2.5}$ or $PM_{10}$ in Zürich (about 7–31%; Szidat et al., 2006), Göteborg (about 12%; Szidat et al., 2009), Birmingham (about 8–11%; Heal et al., 2011), and Beijing (about 13–20%; Sun et al., 2012). Thus, higher WIRC $^{14}C$ pMC at WLG can be interpreted as more bioaerosols with sizes larger than 2.5 or 10.0 μm, such as pollen grains (Pavuluri et al., 2013). Our WIRC $^{14}C$ pMC value is close to soot carbon (68 ± 6)%, but higher than EC $^{14}C$ pMC (45 ± 8)% measured for the Maldives and India (Gustafsson et al., 2009). These comparisons suggested that contemporary-carbon comprises a high fraction of TSP carbonaceous aerosols at this GAW site.

To investigate the WIRC $^{14}C$ pMC variation in detail, weekly-average variations of $^{14}C$ pMC, relative humidity (RH), and mass

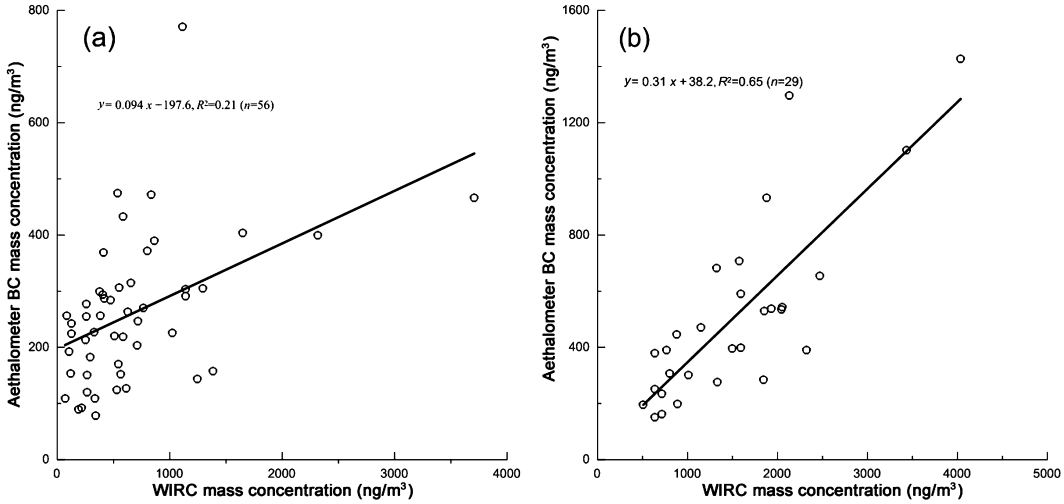


**Fig. 4.** Mass concentrations of aethalometer BC and WIRC extracted from the sampled filters at WLG: (a) for the first period with filter cutting and (b) for the second period without cutting.

**Table 4**
Comparison of $^{14}C$ pMC of WIRC at WLG with other China sites.

| Sites | $^{14}C$ pMC (%) | | | Reference |
|---|---|---|---|---|
| | Average ± Std | (Min–max) | Number | |
| WLG (spring)[a]-remote | 64.1 ± 5.7 | 57.5–79.8 | 12 | This study |
| WLG (autumn)[a]-remote | 61.7 ± 5.5 | 56.3–68.1 | 5 | |
| WLG (winter)[a]-remote | 69.9 ± 7.5 | 55–80.8 | 12 | |
| Lhasa (spring)[a]-urbane | 49.0 ± 5.1 | 39–56 | 11 | Huang et al. (2010) |
| Lhasa (summer)[a]-urbane | 44.0 ± 5.9 | 39–54 | 5 | |
| Lhasa (autumn)[a]-urbane | 44.0 ± 7.5 | 35–54 | 6 | |
| Lhasa (winter)[a]-urbane | 57.0 ± 6.0 | 50–70 | 8 | |
| Zhongguancun, Beijing[b]-urbane | 28 | 33–48 | 8 | Yang et al. (2005) |
| Yufa near Beijing (winter)[b]-rural | 35 | 30–38 | 12 | Sun et al. (2012) |
| Yufa near Beijing (summer)[b]-rural | 39 | 31–44 | 12 | |

[a] WIRC extracted from TSP.
[b] $PM_{2.5}$ carbonaceous particles.

concentrations of TSP and WIRC are shown in Fig. 5(a) and (b) show an anti-correlation between $^{14}C$ pMC and RH, with decreases in $^{14}C$ pMC corresponding to increases in RH, and vice versa (i.e., see weeks #2 to #4, #6 and #7, #11 to #13, #24 and #25). Changes in RH are related to the alternation of air parcels, with more moist parcels originating from east or southeast of WLG, from more populated regions with higher fractions of fossil fuel derived WIRC. Conversely, drier air parcels originate from the more remote west to southwest highlands, with less polluted air masses and higher $^{14}C$ pMC values.

For the first 14 samples, the linearly squared correlation coefficient between $^{14}C$ pMC and RH is 0.65. However, after sample #14, little correlation is evident, suggesting that $^{14}C$ pMC is insensitive to RH over this period; this cannot simply be related to changes in transport paths. We believe continuous fossil fuel combustion heating in Lanzhou and Xining, or towns along the Yellow River canyon, is the primary reason for the reduction in $^{14}C$ pMC in winter and spring. Furthermore, small amounts of atmospheric water vapor during the winter and spring preclude RH as a sensitivity flag for atmospheric transport.

There were two mass concentration peaks for TSP and WIRC: sample #21 (March 14–21, 2006) and sample #24 (April 4–11, 2006). Sample #21 has a lower $^{14}C$ pMC than sample #24,

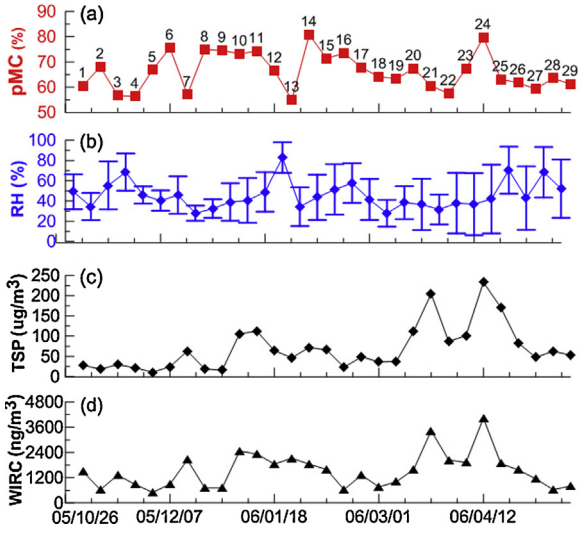


**Fig. 5.** Week-to-week variations of $^{14}C$ pMC (a), RH with standard error (b), TSP (c), and aerosol WIRC (d) mass concentrations from 26 October 2005 to 17 May 2006. Numbers labeled in Fig. 5(a) indicate the serial number of the weeks since 26 October 2005.

suggesting that air parcels traveled through an area with more fossil fuel combustion before collection. Seven-day backward trajectory calculations indicate that indeed these air parcels passed over the highly urbanized Yellow River canyon region (March 17). For sample #24, the backward trajectory shows that most air parcels traveled through the relatively less urbanized area, northwest of WLG. Highest mass concentrations of TSP and WIRC for sample #24 are instead characteristics of a dust storm, rather than fossil fuel derived aerosol transport. These examples illustrate that $^{14}C$ pMC at WLG was very sensitive to changes in regional transport path, even when WIRC or TSP levels remained high.

We noticed a pronounced jump in $^{14}C$ pMC values between sample #13 (January 18–25, 2006) and #14. This was associated with changes in transport path, with air masses from January 19–22, 2006 coming from east of WLG. Such westward transport caused $^{14}C$ pMC to decrease to a minimum value in sample #13. Interestingly, this event was associated with high $^{210}Pb$ concentrations, around 5.81 mBq/m$^3$ (data not shown). A similarly high $^{210}Pb$ activity concentration associated with pollutant transport from the east was evident in the 2003 data (Zheng, Wan, Chan, & Tang, 2008). Almost all the backward trajectories for sample #14 were from the west, especially from the more remote south-west highland areas.

## Summary and conclusions

We present mass concentrations, $\delta^{13}C$ PDB values for WIRC extracted from 79 TSP samples collected on a weekly basis at Mt. Waliguan, a WMO-GAW site in west China. $^{14}C$ pMC values for 29 samples collected in winter and spring were also measured. We estimated uncertainties for these measurements, showing that the sampling and pretreatment techniques were significant factors contributing to underestimation of WIRC mass concentrations. The mass concentrations for WIRC were compared with aethalometer BC measurements. Our study revealed that:

(i) The overall average mass concentration of WIRC in the 79 week-long samples was about (1183 ± 120) ng/m$^3$, and the relative ratio to TSP was (2.25 ± 1.3)%. A seasonal cycle to WIRC mass concentration was evident; lower values in the summer to autumn period were associated with a higher WIRC/TSP mass ratio; while the opposite trend occurred in winter to spring. Although mass concentration changes were similar for both WIRC and BC measurements, WIRC mass concentrations were higher because of high TSP loadings in winter and spring.
(ii) $C_3$ plant or fossil fuel combustion appears to be the main sources for WIRC at WLG, as suggested by their $\delta^{13}C$ value of (−25.3 ± 0.8)‰ ($n$ = 79). Seasonal variation in $\delta^{13}C$ values was

not marked. Summer to autumn $\delta^{13}C$ values (−25.4‰) indicated that biofuel (dung) and biomass burning emissions were their dominant sources for WIRC.

(iii) Average $^{14}C$ pMC values were (67.2 ± 7.7)% ($n$ = 29) for late autumn to late spring samples. This $^{14}C$ pMC value was higher than at Lhasa and other urban sites. However, $^{14}C$ pMC at WLG was lower than for $PM_{2.5}$, but higher than values for EC in $PM_{2.5}$ from rural or remote sites. WIRC $^{14}C$ pMC values at WLG provided signatures of different air mass transport paths: higher fractions of fossil fuel derived WIRC in late autumn and early winter were associated with moist air-parcels transported from east of WLG, while air masses transported from the remote highlands located southwest of WLG were characterized by high $^{14}C$ pMC values. High $^{14}C$ pMC values also were recorded during a spring dust storm, with abnormally high mass concentrations of TSP and WIRC. Winter to spring usage of fossil fuels for heating in the region east of WLG had a negative effect on $^{14}C$ pMC values at WLG.

## Acknowledgements

This work was supported by the National Natural Sciences Foundation of China (Grant Nos. 41175115;40830102;40575013 and 40175032). We are grateful to Dr. H.N. Lee from the Environmental Measurements Laboratory, Department of Homeland Security, New York, USA for providing instruments for in situ aerosol sampling. We acknowledge the use of online software available at www.arl.noaa.gov/ready/open/traj.html to determine backward trajectories of aerosol particles.

## References

Bench, G., Fallon, S., Schichtel, B., Malm, W., & McDade, C. (2007). Relative contributions of fossil and contemporary carbon sources to $PM_{2.5}$ aerosols at nine Interagency Monitoring for Protection of Visual Environments (IMPROVE) network sites. *Journal of Geophysical Research: Atmospheres*, *112*, D10205. http://dx.doi.org/10.1029/2006JD007708

Collaud Coen, M., Weingartner, E., Schaub, D., Hueglin, C., Corrigan, C., Henning, S., et al. (2004). Saharan dust events at the Jungfraujoch: Detection by wavelength dependence of the single scattering albedo and first climatology analysis. *Atmospheric Chemistry and Physics*, *4*, 2465–2480.

Currie, L. A., Klouda, G. A., & Cooper, J. A. (1980). Mini-radiocarbon measurements, chemical selectivity, and the impact of man on environmental pollution and climate. *Radiocarbon*, *22*, 347–362.

Ding, P., Shen, C. D., Wang, N., Yi, W. X., Ding, X. F., Fu, D. P., et al. (2010). Carbon isotopic composition, turnover and origins of soil $CO_2$ in a monsoon evergreen broad leaf forest in Dinghushan Biosphere Reservoir, South China. *Chinese Science Bulletin*, *55*(23), 2548–2556.

Draxler, R. R., & Rolph, G. D. (2003). *HYSPLIT (HYbrid Single-Particle Lagrangian Integrated Trajectory) model access via NOAA ARL READY*. Silver Spring, MD, USA: NOAA Air Resources Laboratory. http://www.arl.noaa.gov/ready/hysplit4.html

Gelencsér, A., May, B., Simpson, D., Sánchez-Ochoa, A., Kasper-Giebl, A., Puxbaum, H., et al. (2007). Source apportionment of $PM_{2.5}$ organic aerosol over Europe: Primary/secondary, natural/anthropogenic and fossil/biogenic origin. *Journal of Geophysical Research: Atmospheres*, *112*, D23S04. http://dx.doi.org/10.1029/2006JD008094

Gustafsson, Ö., Kruså, M., Zencak, Z., Sheesley, R. J., Granat, L., Engström, E., et al. (2009). Brown clouds over south Asia: Biomass or fossil fuel combustion? *Science*, *323*, 495–498.

Han, Y. M., Cao, J. J., An, Z. S., Chow, J. C., Watson, J. G., & Jin, Z. D. (2007). Evaluation of the thermal/optical reflectance method for quantification of elemental carbon in sediments. *Chemosphere*, *69*, 526–533.

Heal, M. R., Naysmith, P., Cook, G. T., Xu, S., Duran, T. R., & Harrison, R. M. (2011). Application of $^{14}C$ analyses to source apportionment of carbonaceous PM2.5 in the UK. *Atmospheric Environment*, *45*, 2341–2348.

Hedges, J. I., Eglinton, G., Hatcher, P. G., Kirchman, D. L., Arnosti, C., Derenne, S., et al. (2000). The molecularly-uncharacterized component of nonliving organic matter in natural environments. *Organic Geochemistry*, *31*, 945–958.

Huang, J., Kang, S., Shen, C. D., Cong, Z. Y., Liu, K. X., Wang, W., et al. (2010). Seasonal variations and sources of ambient fossil and biogenic-derived carbonaceous aerosols based on $^{14}C$ measurements in Lhasa, Tibet. *Atmospheric Research*, *96*, 553–559.

Husain, L., Khan, A. J., Ahmed, T., Swami, K., Bari, A., Webber, J. S., et al. (2008). Trends in atmospheric elemental carbon concentrations from 1835 to 2005. *Journal of Geophysical Research: Atmospheres*, *113*, D13102. http://dx.doi.org/10.1029/2007JD009398

Khan, A. J., Swami, K., Ahmed, T., Bari, A., Shareef, A., & Husain, L. (2009). Determination of elemental carbon in lake sediments using a thermal–optical transmittance (TOT) method. *Atmospheric Environment*, *43*, 5989–5995.

Kivekäs, N., Sun, J., Zhan, M., Kerminen, V. M., Hyvärinen, A., Komppula, M., et al. (2009). Long term particle size distribution measurements at Mount Waliguan, a high-altitude site in inland China. *Atmospheric Chemistry and Physics*, *9*, 5461–5474.

Kuhn, T., Damoah, R., Bacak, A., & Sloan, J. J. (2010). Characterising aerosol transport into the Canadian High Arctic using aerosol mass spectrometry and Lagrangian modeling. *Atmospheric Chemistry and Physics*, *10*, 10489–10502.

Lee, H. N., Wan, G., Zheng, X., Sanderson, C. G., Josse, B., Wang, S., et al. (2004). Measurements of $^{210}Pb$ and $^{7}Be$ in China and their analysis accompanied with global model calculations of $^{210}Pb$. *Journal of Geophysical Research: Atmospheres*, *109*, D22203. http://dx.doi.org/10.1029/2004JD005061

Levin, I., Hammer, S., Kromer, B., & Meinhardt, F. (2008). Radiocarbon observations in atmospheric $CO_2$: Determining fossil fuel $CO_2$ over Europe using Jungfraujoch observations as background. *Science of the Total Environment*, *391*, 211–216.

Li, J., Khan, A. J., & Husain, L. (2002). A technique for determination of black carbon in cellulose filters. *Atmospheric Environment*, *36*, 4699–4704.

Li, S.-M., Tang, J., Xue, H. S., & Toom-Sauntry, D. (2000). Size distribution and estimated optical properties of carbonate, water-soluble organic carbon and sulfate in aerosols at a remote high altitude site in western China. *Geophysical Research Letters*, *27*, 1107–1110.

Liu, K., Ding, X., Fu, D., Pan, Y., Wu, X., Guo, Z., et al. (2007). A new compact AMS system at Peking University. *Nuclear Instruments and Methods in Physics Research Section B*, *259*, 23–26.

Ma, J., Tang, J., Li, S.-M., & Jacobson, M. Z. (2003). Size distributions of ionic aerosols measured at Waliguan Observatory: Implication for nitrate gas-to-particle transfer processes in the free troposphere. *Journal of Geophysical Research: Atmospheres*, *108*(D17), 4541. http://dx.doi.org/10.1029/2002JD003356

Novakov, T., & Penner, J. E. (1993). Large contribution off organic aerosols to cloud-condensation-nuclei concentration. *Nature*, *365*, 823–8261.

Pavuluri, C. M., Kawamura, K., Swaminathan, T., & Tachibana, E. (2011). Stable carbon isotopic compositions of total carbon, dicarboxylic acids and glyoxylic acid in the tropical Indian aerosols: Implications for sources and photochemical processing of organic aerosols. *Journal of Geophysical Research: Atmospheres*, *116*, D18307. http://dx.doi.org/10.1029/2011JD015617

Pavuluri, C. M., Kawamura, K., Uchida, M., Kondo, M., & Fu, P. (2013). Enhanced modern carbon and biogenic organic tracers in Northeast Asian aerosols during spring/summer. *Journal of Geophysical Research: Atmospheres*, *118*, 2362–2371.

Saxena, P., & Hildemann, L. M. (1996). Water-soluble organics in atmospheric particles: A critical review of the literature and application of thermodynamics to identify candidate compounds. *Journal of Atmospheric Chemistry*, *24*, 57–109.

Schichtel, B. A., Malm, W. C., Bench, G., Fallon, S., McDade, C. E., Chow, J. C., et al. (2008). Fossil and contemporary fine particulate carbon fractions at 12 rural and urban sites in the United States. *Journal of Geophysical Research: Atmospheres*, *113*, D02311. http://dx.doi.org/10.1029/2007JD008605

Shen, C. D., Liu, D. S., Peng, S. L., Sun, Y. M., Jiang, M. T., Yi, W. X., et al. (1999). $^{14}C$ measurement of forest soils in Dinghushan Biosphere Reserve. *Chinese Science Bulletin*, *44*(3), 251–256.

Sun, X. S., Hu, M., Guo, S., Liu, K. X., & Zhou, L. P. (2012). $^{14}C$-based source assessment of carbon carbonaceous aerosols at a rural site. *Atmospheric Environment*, *50*, 36–40.

Szidat, S., Jenk, T. M., Gäggeler, H. W., Synal, H. A., Fisseha, R., Baltensperger, U., et al. (2004). Radiocarbon ($^{14}C$)-deduced biogenic and anthropogenic contributions to organic carbon (OC) of urban aerosols from Zürich, Switzerland. *Atmospheric Environment*, *38*, 4035–4044.

Szidat, S., Jenk, T. M., Synal, H. A., Kalberer, M., Wacker, L., Hajdas, I., et al. (2006). Contributions of fossil fuel, biomass-burning, and biogenic emissions to carbonaceous aerosols in Zurich as traced by $^{14}C$. *Journal of Geophysical Research: Atmospheres*, *111*, D07206. http://dx.doi.org/10.1029/2005JD006590

Szidat, S., Ruff, M., Perron, N., Wacker, L., Synal, H., Hallquist, M., et al. (2009). Fossil and non-fossil sources of organic carbon (OC) and elemental carbon (EC) in Goeteborg, Sweden. *Atmospheric Chemistry and Physics*, *9*, 1521–1535.

Tang, J., Wen, Y. P., Zhou, L. X., Qi, D., Zheng, M., Neil, T., et al. (1999). The observational Study of black carbon in clean air area of western China. *Quarterly Journal of Applied Meteorology*, *10*(2), 160–170 (in Chinese).

Wen, Y. P., Xu, X. B., Tang, J., Zhang, X. C., & Zhao, Y. C. (2001). Enrichment characteristics and origin of atmospheric aerosol elements at Mt. Waliguan. *Quarterly Journal of Applied Meteorology*, *12*(4), 400–408 (in Chinese).

Xue, L. K., Wang, T., Zhang, J. M., Zhang, X. C., Poon, C. N., Ding, A. J., et al. (2011). Source of surface ozone and reactive nitrogen speciation at Mount Waliguan in western China: New insights from the 2006 summer study. *Journal of Geophysical Research: Atmospheres*, *116*, D07306. http://dx.doi.org/10.1029/2010JD014735

Yang, F., He, K., Ye, B., Chen, X., Cha, L., Cadle, S. H., et al. (2005). One-year record of organic and elemental carbon in fine particles in downtown Beijing and Shanghai. *Atmospheric Chemistry and Physics*, *5*, 1449–1457.

Zheng, X. D., Wan, G. J., Chan, C. Y., & Tang, J. (2008). Measurement and meteorological analysis of $^{7}Be$ and $^{210}Pb$ in aerosol at Waliguan Observatory. *Advances in Atmospheric Sciences*, *25*(3), 404–416.